Evidence for prolate structure in light Pb isotopes from in-beam γ-ray spectroscopy of ^{185}Pb

J. Pakarinen,[1,2,*] A. N. Andreyev,[3,4] R. Julin,[1] S. Juutinen,[1] S. Antalic,[5] L. Bianco,[2] I. G. Darby,[2,†] S. Eeckhaudt,[1] T. Grahn,[1,2]
P. T. Greenlees,[1] D. G. Jenkins,[6] P. Jones,[1] P. Joshi,[6] H. Kettunen,[1] M. Leino,[1] A.-P. Leppänen,[1,‡] P. Nieminen,[1,7] M. Nyman,[1]
R. D. Page,[2] J. Perkowski,[1,§] P. M. Raddon,[6] P. Rahkila,[1] D. Rostron,[2] J. Saren,[1] C. Scholey,[1] J. Sorri,[1] B. Streicher,[4]
J. Uusitalo,[1] K. Van de Vel,[1,‖] M. Venhart,[1,¶] R. Wadsworth,[6] and D. R. Wiseman[2]

[1]*Department of Physics, University of Jyväskylä, P. O. Box 35, 40014 Jyväskylä, Finland*
[2]*Department of Physics, Oliver Lodge Laboratory, University of Liverpool, Liverpool, L69 7ZE, United Kingdom*
[3]*TRIUMF, 4004 Wesbrook Mall, Vancouver, British Columbia, Canada V6T 2A3*
[4]*Instituut voor Kern- en Stralingsfysica, K. U. Leuven, B-3001 Leuven Belgium*
[5]*Department of Nuclear Physics and Biophysics, Comenius University, Bratislava, SK-84248, Slovakia*
[6]*Department of Physics, University of York, Heslington, York, YO10 5DD, United Kingdom*
[7]*Department of Nuclear Physics, R. S. Phys. S. E., Australian National University, Canberra, A.C.T. 0200, Australia*
(Received 13 May 2009; published 24 September 2009)

For the first time, excited states in ^{185}Pb have been observed in in-beam γ-ray spectroscopic measurements using the recoil-decay tagging method. The resulting level scheme reveals a strongly coupled yrast band structure that originates from coupling of the $i_{13/2}$ quasineutron to a prolate deformed core. The band is also observed to de-excite via the spherical α-decaying $13/2^+$ isomeric state.

A considerable body of both theoretical and experimental evidence has been gathered for coexisting configurations possessing different shapes in the very neutron deficient Pb isotopes [1,2]. This phenomenon becomes particularly apparent in Pb isotopes in the vicinity of the $N = 104$ neutron midshell, where the competing deformed structures intrude down to energies close to the spherical ground state. The intruder states have been associated with proton multiparticle-multihole excitations across the closed $Z = 82$ shell [3–5]. This picture is supported by hindrance factors obtained in α-decay fine-structure studies [6]. Mean-field calculations suggest that each intruder configuration can be associated with a different shape [7–11]. Together with the spherical ground state, they result in a unique triplet of shape-coexisting 0^+ states in ^{186}Pb [12].

In in-beam γ-ray studies via fusion-evaporation reactions, rotational yrast bands have been observed in even-mass $^{182-188}$Pb nuclei [13–16]. The moments of inertia of these bands resemble those of yrast bands in even-mass Hg isotones and they have been associated with the prolate minimum [1,2]. Candidates for oblate non-yrast bands have also been seen in ^{186}Pb and ^{188}Pb [15,16]. Recently, lifetime measurements have provided more information concerning the collectivity

and deformation of the yrast bands in ^{186}Pb and ^{188}Pb [17,18], but more evidence regarding their shape is still needed.

Information about the shape of the midshell Pb nuclei can be obtained by probing band structures in their neighboring odd-mass nuclei. The coupling of the odd quasiparticle to the even-even core results in a characteristic level pattern, depending on the shape of the core nucleus. So far, in odd-A Pb isotopes of $A > 189$, yrast structures have been associated with weak coupling of an $i_{13/2}$ neutron hole to the yrast states of the neighboring nearly spherical even-A nucleus [19–25]. In ^{189}Pb, the yrast states are associated with the spherical shape, but strong mixing with the prolate states is indicated by $E0$ contributions observed in transitions between levels of the same spin and parity. In the same nucleus, a non-yrast band structure has been observed in the decay of a high-spin isomer and associated with the strong coupling of the $i_{13/2}$ quasineutron to the shape-coexisting prolate core [19]. For ^{187}Pb, two alternative explanations were given by Baxter *et al.*, who associated the observed yrast states with the weak coupling of the $i_{13/2}$ quasineutron to the spherical core or with the favored signature states resulting from the strong coupling of this neutron to the shape-coexisting prolate core. In the study of ^{187}Bi and ^{189}Bi isotopes, the $\frac{1}{2}^+$[660] odd proton was found to be decoupled from the prolate deformed even-even Pb core [26], whereas in heavier ^{191}Bi and ^{193}Bi isotopes oblate strongly coupled bands based on the $\frac{13}{2}^+$[606] orbital have been observed [27]. Thus, the investigation of ^{185}Pb can provide important direct evidence on nuclear shape in the Pb isotopes around the $N = 104$ neutron midshell through the character of particle-core coupling [28].

Fusion-evaporation reactions can be employed to populate excited states in midshell Pb nuclei. However, due to the small production cross sections and other competing reaction channels, especially fission, in-beam spectroscopic studies are only possible when employing the recoil-decay tagging

---

*[*]janne.pakarinen@cern.ch; present address: ISOLDE, CERN, Geneva, Switzerland.

[†]Present address: Department of Physics and Astronomy, University of Tennessee, Knoxville, Tennessee 37996, USA.

[‡]Present address: Northern Finland Regional Laboratory, STUK-Radiation and Nuclear Safety Authority, Rovaniemi, Finland.

[§]Present address: Division of Nuclear Physics, University of Lódz, 90-236 Lódz, Poland.

[‖]Present address: VITO, IMS, Mol, Belgium.

[¶]Present address: Department of Nuclear Physics and Biophysics, Comenius University, Bratislava, SK-84248, Slovakia.

(RDT) technique [29,30]. In the present work, an in-beam γ-ray spectroscopic study of ^{185}Pb has been carried out by employing the gas-filled recoil separator RITU [31] and the associated detector systems dedicated to RDT experiments at the Accelerator Laboratory of the University of Jyväskylä (JYFL), Finland.

Data from two different in-beam experiments were collected. The ^{82}Kr + ^{106}Pd and ^{83}Kr + ^{104}Pd reactions were used with ^{82}Kr and ^{83}Kr beams of 367 and 362 MeV, respectively, extracted from the JYFL cyclotron. The irradiation time was 6 days in both experiments. The first experiment was optimized for ^{185}Pb produced via the $3n$-fusion evaporation channel, whereas in the second experiment (dedicated to a study of ^{184}Pb), ^{185}Pb was produced as a side product via the $2n$ channel. Cross sections of ≈ 110 μb and ≈ 30 μb, respectively, were deduced for the $13/2_1^+$ α-decaying state. During both experiments the beam intensity was limited to ≈ 6 pnA by the counting rates of the γ-ray detectors at the target area, resulting in total counting rates of ≈ 250 Hz at the focal-plane implantation detector. The α-decay half-life, energy, and branching ratio measured earlier for the excited $13/2_1^+$ state in ^{185}Pb are 4.3 s, 6408 keV, and 50%, respectively [32].

Prompt γ rays were detected using the JUROGAM Ge detector array consisting of 43 Compton-suppressed single-crystal Ge detectors. The total photo-peak efficiency of this array for 1332 keV γ rays is 4.2%. The recoiling fusion-evaporation residues were separated in-flight from the beam using the gas-filled recoil separator RITU and implanted into a pair of double-sided silicon strip detectors (DSSSDs) of the GREAT focal-plane detection system [33]. In the DSSSDs, the energy of implanted recoils and their subsequent α decay were measured. Upstream of the DSSSDs, a multiwire proportional counter was used to extract energy loss of recoils and together with the DSSSD it allowed time-of-flight information to be deduced.

The energies of events occurring in all detectors were recorded by the triggerless total data readout data acquisition system and time-stamped using a 100-MHz clock [34]. Subsequent temporal and spatial correlations between the various detector groups were performed using the GRAIN data analysis package [35]. The high granularity of the DSSSDs (4800 pixels) enabled the RDT method to be used for ^{185}Pb, where the half-life of the α-decaying state is of the order of 5 s.

Prompt γ rays detected in coincidence with an implanted recoil and followed by a subsequent ^{185}Pb α decay in the same DSSSD pixel within 13 s were selected in the data analysis. The analysis of the data was completed with the RADWARE software package [36].

In Fig. 1, the α-particle energy spectra correlated with implanted recoils from both experiments are shown. Variations arise from the slightly different reactions. During 300 h of effective beam time, a total of 10^5 events associated with the α decay of the $13/2_1^+$ isomeric state in ^{185}Pb were recorded. Due to the fragmented decay structure and overlapping α-decay energies with ^{186}Pb, the decay of the $3/2^-$ state could not be employed for RDT $\gamma\gamma$-coincidence analysis. Thus the present work concentrates only on the RDT study of the $13/2_1^+$ isomeric state.
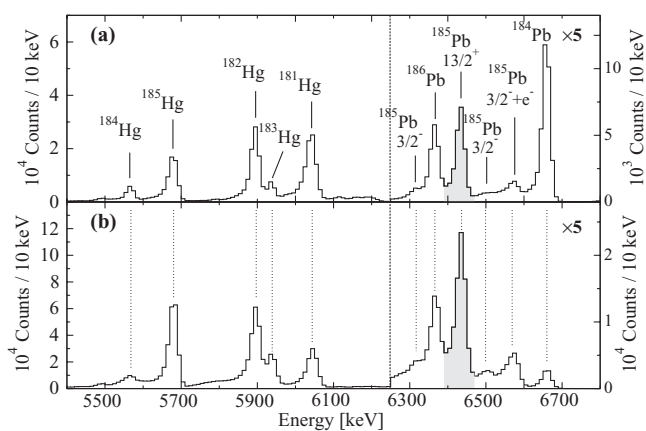

FIG. 1. Energy spectra of α particles measured in the DSSSDs of the GREAT spectrometer correlated with implanted recoils within a search time of 13 s. The spectrum (a) is from the ^{83}Kr + ^{104}Pd reactions and spectrum (b) from the ^{82}Kr + ^{106}Pd reactions. The shaded areas correspond to energy gates used for tagging and the energy range between 6250 and 6800 keV has been magnified (by factor of 5) for illustration purposes.

Figure 2(a) shows the recoil-gated singles γ-ray energy spectrum correlated with the α decay of the $13/2_1^+$ state in ^{185}Pb. The strongest transitions can be firmly assigned to ^{185}Pb, but the existence of contaminant transitions originating from ^{185}Tl, ^{182}Hg, and ^{184}Hg nuclei produced via yp-xn and α-xn fusion-evaporation channels is apparent. This contamination arises from random correlations with recoils implanted into the same pixel of the DSSSD between implantation and
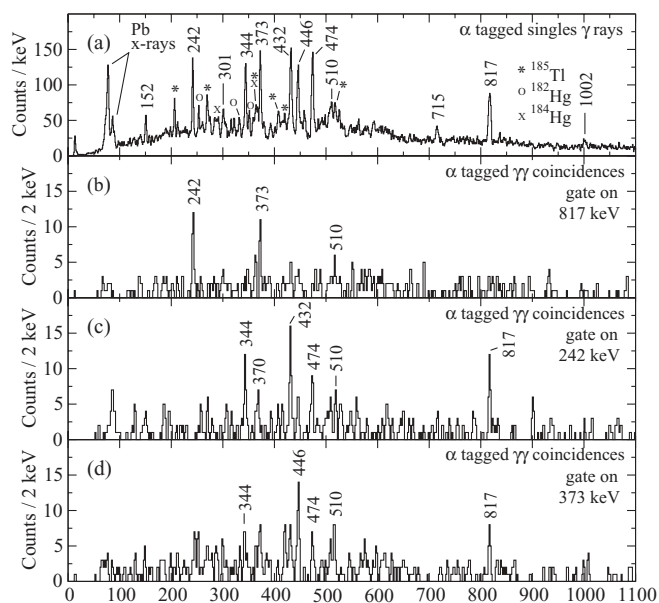

FIG. 2. (a) Singles γ-ray energy spectrum gated with recoils and tagged with α decays of the $13/2_1^+$ state in ^{185}Pb. [(b), (c), and (d)] Recoil-gated, α-tagged $\gamma\gamma$ coincidence spectra with a gate on the 817-, 242-, and 373-keV transitions, respectively. Transitions associated with ^{185}Pb are labeled with energies, whereas contaminant transitions are marked with *, o, and x for ^{185}Tl, ^{182}Hg, and ^{184}Hg, respectively.

TABLE I. The γ-ray transitions measured in the present γ-ray energy, relative γ-ray intensity, and tentatively assigned spins are listed.

E_γ (keV)	$I_{\rm rel}$	$I_i^\pi \rightarrow I_f^\pi$
151.8(3)	15(3)	–
242.0(3)	39(5)	$(19/2_1^+) \rightarrow (17/2_1^+)$
301.4(4)	12(3)	$(23/2_1^+) \rightarrow (21/2_1^+)$
344(1)	15(10)	$(19/2_1^+) \rightarrow (15/2_1^+)$
344.2(3)	36(10)	$(17/2_1^+) \rightarrow (13/2_2^+)$
370(1)	<10	–
372.8(3)	60(7)	$(21/2_1^+) \rightarrow (17/2_1^+)$
432.1(3)	76(9)	$(23/2_1^+) \rightarrow (19/2_1^+)$
445.8(3)	61(8)	$(25/2_1^+) \rightarrow (21/2_1^+)$
473.9(3)	73(9)	$(13/2_2^+) \rightarrow 13/2_1^+$
509.7(6)	26(6)	$(27/2_1^+) \rightarrow (23/2_1^+)$
715.4(6)	24(5)	$(15/2_1^+) \rightarrow 13/2_1^+$
817.3(6)	100(10)	$(17/2_1^+) \rightarrow 13/2_1^+$
1002(2)	16(5)	–

subsequent decay of the nuclei of interest. Fortunately, the contaminant nuclei are rather well known and they do not have many overlapping transitions with the transitions assigned to ^{185}Pb. In Table I, γ rays associated with the $13/2_1^+$ state in ^{185}Pb are listed.

The collected RDT $\gamma\gamma$ coincidence data were sufficient to place most of the observed transitions into the level scheme. In Figs. 2(b)–2(d), a selection of recoil-gated, α-tagged $\gamma\gamma$ coincidence spectra are shown. Based on coincidence relations, intensity balances and energy-sum arguments, the partial level scheme shown in Fig. 3 was constructed. Due to insufficient statistics, γ-ray angular distribution information could not be obtained. Thus, the level spin and parity assignments are only tentative.

Analogous to the 831-keV state in ^{187}Pb [20], the 817-keV transition is assigned to feed the $13/2_1^+$ isomeric state and the initial state is assigned as $17/2_1^+$. As shown in Fig. 2(b), the 817-keV transition is in coincidence with two γ rays at 242 and 373 keV. As the $13/2_1^+$ state de-excites only via α decay, these two γ rays are set to populate the $17/2_1^+$ state.

The coincidence relation between the 817-keV transition and the transitions at 242 and 373 keV is confirmed in the spectra shown in Figs. 2(c) and 2(d). They also prove that the 242- and 373-keV transitions do not form a cascade. Thus, they are set to feed the $17/2_1^+$ state and their parent states are assigned as $19/2_1^+$ and $21/2_1^+$, respectively.

Another common feature in the spectra shown in Figs. 2(c) and 2(d) are the transitions at 344 and 474 keV, which are in mutual coincidence and sum up to 818 keV. Because they do not coincide with the 817-keV transition, they are considered an alternative de-excitation path for the 818-keV state. The ordering of this cascade is deduced on the basis of intensity balance arguments. The 474-keV state is assigned as $13/2_2^+$. The assignment is also supported by the non-observation of the 586- and 1060-keV transitions (which would have multipole order higher than 2) from the $19/2_1^+$ state.

The transitions feeding the $19/2_1^+$ and $21/2_1^+$ states can be seen in Figs. 2(c) and 2(d). The 432- and 510-keV transitions form a cascade feeding the $19/2_1^+$ state, whereas the 446-keV transition populates the $21/2_1^+$ state. Other transitions, not discussed here, were placed into the level scheme based on similar considerations. The isomeric α decaying $13/2_1^+$ state in ^{185}Pb presumably represents a coupling of the $i_{13/2}$ quasineutron to the spherical ground state of the even-mass Pb core [32].

The level scheme above the 474-keV $13/2_2^+$ state clearly resembles a strongly coupled rotational band with $E2$ cascades above the $13/2_2^+$ and $15/2_1^+$ states connecting levels of favored and unfavored signatures, respectively. The non-observation of transitions from favored to unfavored states can be explained by relatively large internal conversion due to small transition energies.

A quadrupole deformation parameter $\beta_2 = 0.29$ is extracted from the lifetime measurements for the suggested prolate yrast band in ^{186}Pb [17]. The oblate band is expected to represent a less deformed shape of $\beta_2 \approx -0.15$ [8,15]. Within the framework of the Nilsson model, both at the prolate and oblate side, the odd neutron occupies the $\frac{7}{2}^+[633]$ (or $\frac{9}{2}^+[624]$) orbital of $i_{13/2}$ origin. It can be expected that coupling of this neutron to a prolate core results in a strongly coupled band,
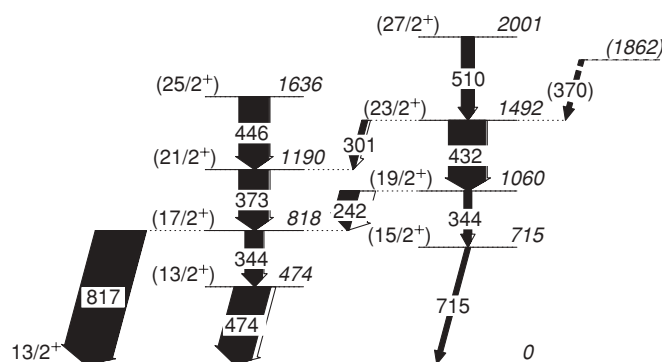

FIG. 3. Proposed level scheme of ^{185}Pb deduced from the present data. The widths of the arrows are proportional to the measured γ-ray intensities. The level energies are relative to the $13/2_1^+$ isomeric state.
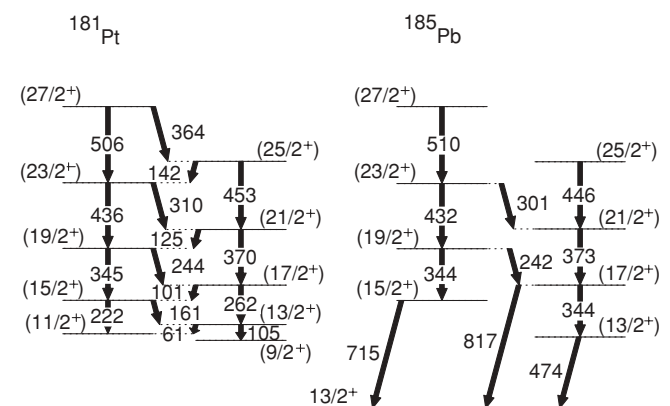

FIG. 4. Comparison between the proposed strongly coupled bands in ^{185}Pb and ^{181}Pt. Level schemes have been lined up with the $17/2_1^+$ levels.
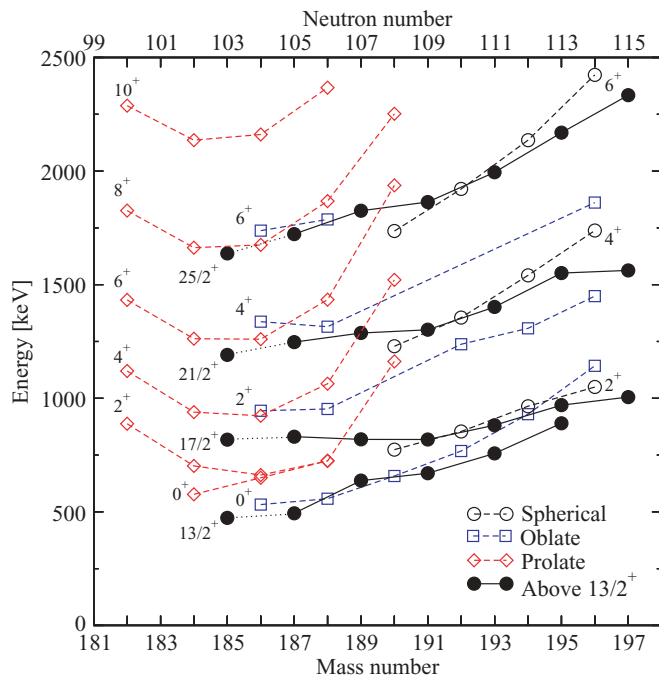
FIG. 5. (Color online) Level energy systematics for Pb isotopes. In the odd-mass isotopes, the level energies of favored states are shown relative to the $13/2_1^+$ isomeric state. Data are taken from the present work, Refs. [2,16,19–22,43–52], and references therein.

whereas coupling to a less-deformed oblate core may lead to a decoupled band structure [28]. The strong coupling scheme is supported by the level scheme of Fig. 3.

In fact, there are remarkable similarities between the observed band structure in ^{185}Pb and the strongly coupled prolate bands seen in Hg and Pt isotopes in the vicinity of the $N = 104$ midshell, see, e.g., Refs. [37–41]. As an example, in Fig. 4 ^{185}Pb is compared with its isotone ^{181}Pt [39], where the prolate-oblate mixing is not as pronounced as in Hg isotopes [42]. As shown in Fig. 4, the transition energies above the $15/2_1^+$ state are almost identical.

A $B(M1; I \rightarrow I - 1)/B(E2; I \rightarrow I - 2)$ ratio of $0.06(2)\mu_N^2/e^2b^2$ was extracted for the de-excitation of the $I^\pi = 23/2_1^+$ level. The value is roughly consistent with the corresponding value in ^{181}Pt $(0.14(2)\mu_N^2/e^2b^2)$ [39] and is also in accord with the value deduced for ^{185}Hg $(\sim 0.1\mu_N^2/e^2b^2)$ [38].

The band in ^{181}Pt shown in Fig. 4 has been associated with the $\frac{9}{2}^+$[624] Nilsson orbital and is seen down to the $9/2^+$ level. In ^{185}Pb such non-yrast levels below the $13/2_2^+$ level may well be bypassed by high-energy transitions to the $13/2_1^+$ state. The signature splitting in these bands in ^{185}Pb and ^{181}Pt are

similar. In Ref. [39] it is associated with admixture of a low-Ω component or with triaxiality.

The present data show that in ^{185}Pb the $B(E2; 17/2_1^+ \rightarrow 13/2_2^+)$ strength is approximately 30 times higher than for the $17/2_1^+ \rightarrow 13/2_1^+$ transition supporting suggestion that the $13/2_2^+$ state is a member of the prolate band. Compared to the similar band in the isotone ^{181}Pt, the energy of the $13/2_2^+$ state is lower than that expected from the regular rotational band structure. This lowering could be due to mixing with the (unobserved) oblate $13/2^+$ state.

In Fig. 5 systematics of some yrast levels in neutron deficient Pb isotopes are shown. The near-degeneracy of level energies between the even- and odd-A Pb isotopes for $A \geqslant 191$ reveals the weak coupling of the $i_{13/2}$ quasineutron to a spherical core [21–25]. In isotopes with $A \leqslant 189$ this degeneracy is broken as the yrast $17/2^+$, $21/2^+$, and $25/2^+$ levels lie higher than the yrast 2^+, 4^+, and 6^+ levels, respectively, which is typical of a change toward a strong coupling scheme [53]. As discussed in the introduction, possible strongly coupled structures have been observed in ^{189}Pb and ^{187}Pb, though the band in ^{187}Pb could also be interpreted as weak coupling of the $i_{13/2}$ quasineutron. The strongly coupled picture is supported by the present observation of the prolate band in ^{185}Pb. It should be noted that a 472-keV $13/2_2^+$ state in ^{187}Pb is seen in the α-decay study by Andreyev *et al.* and associated with the prolate shape [54].

In summary, excited states in ^{185}Pb have been observed for the first time in RDT in-beam γ-ray measurements and a tentative level scheme above the $13/2_1^+$ isomeric state has been established. The structure for states above spin 15/2 is suggested to be a strongly coupled band based on the $\frac{9}{2}^+$[624] orbital, similar to that described by Baxter *et al.* [20]. The level energy of the $13/2_2^+$ state is lower than that expected from the observed band, suggesting the presence of the close-lying (unobserved) oblate $13/2^+$ state. Consequently, the present data provide direct evidence for prolate deformation in Pb isotopes near the $N = 104$ neutron midshell.

[1] J. L. Wood, K. Heyde, W. Nazarewicz, M. Huyse, and P. Van Duppen, Phys. Rep. **215**, 101 (1992).

[2] R. Julin, K. Helariutta, and M. Muikku, J. Phys. G: Nucl. Part. Phys. **27**, R109 (2001).

[3] P. Van Duppen *et al.*, Phys. Rev. Lett. **52**, 1974 (1984).

[4] P. Van Duppen, M. Huyse, K. Heyde, and J. L. Wood, J. Phys. G: Nucl. Part. Phys. **16**, 441 (1990).

[5] K. Heyde, J. Schietse, and C. De Coster, Phys. Rev. C **44**, 2216 (1991).

[6] P. Van Duppen and M. Huyse, Hyperfine Interact. **129**, 149 (2000).

[7] F. R. May, V. V. Pashkevich, and S. Frauendorf, Phys. Lett. **B68**, 113 (1977).

[8] W. Nazarewicz, Phys. Lett. **B305**, 195 (1993).

[9] R. R. Rodríguez-Guzmán, J. L. Egido, and L. M. Robledo, Phys. Rev. C **69**, 054319 (2004).

[10] M. Bender, P. Bonche, T. Duguet, and P.-H. Heenen, Phys. Rev. C **69**, 064303 (2004).

[11] V. Hellemans, R. Fossion, S. D. Baerdemacker, and K. Heyde, Phys. Rev. C **71**, 034308 (2005).

[12] A. N. Andreyev *et al.*, Nature **405**, 430 (2000).

[13] D. G. Jenkins *et al.*, Phys. Rev. C **62**, 021302(R) (2000).

[14] J. F. C. Cocks *et al.*, Eur. Phys. J. A **3**, 17 (1998).

[15] J. Pakarinen *et al.*, Phys. Rev. C **75**, 014302 (2007).

[16] G. D. Dracoulis *et al.*, Phys. Rev. C **69**, 054318 (2004).

[17] T. Grahn *et al.*, Phys. Rev. Lett. **97**, 062501 (2006).

[18] T. Grahn *et al.*, Nucl. Phys. **A801**, 83 (2008).

[19] A. M. Baxter *et al.*, Phys. Rev. C **71**, 054302 (2005).

[20] A. M. Baxter *et al.*, Phys. Rev. C **58**, 2671 (1998).

[21] N. Fotiades *et al.*, Phys. Rev. C **57**, 1624 (1998).

[22] J. M. Lagrange, M. Pautrat, J. S. Dionisio, Ch. Vieu, and J. Vanhorenbeeck, Nucl. Phys. **A530**, 437 (1991).

[23] M. Pautrat, J. M. Lagrange, A. Virdis, J. S. Dionisio, Ch. Vieu, and J. Vanhorenbeeck, Phys. Scr. **34**, 378 (1998).

[24] G. Baldsiefen *et al.*, Nucl. Phys. **A574**, 521 (1994).

[25] S. Chmel, F. Brandolini, R. V. Ribas, G. Baldsiefen, A. Görgen, M. De Poli, P. Pavan, and H. Hübel, Phys. Rev. Lett. **79**, 2002 (1997).

[26] A. Hürstel *et al.*, Eur. Phys. J. A **21**, 365 (2004).

[27] P. Nieminen *et al.*, Phys. Rev. C **69**, 064326 (2004).

[28] K. Heyde, P. Van Isacker, M. Waroquier, J. L. Wood, and R. A. Meyer, Phys. Rep. **102**, 291 (1983).

[29] K.-H. Schmidt *et al.*, Phys. Lett. **B168**, 39 (1986).

[30] E. S. Paul *et al.*, Phys. Rev. C **51**, 78 (1995).

[31] M. Leino *et al.*, Nucl. Instrum. Methods B **99**, 653 (1995).

[32] A. N. Andreyev *et al.*, Eur. Phys. J. A **14**, 63 (2002).

[33] R. D. Page *et al.*, Nucl. Instrum. Methods B **204**, 634 (2003).

[34] I. H. Lazarus *et al.*, IEEE Trans. Nucl. Sci. **48**, 567 (2001).

[35] P. Rahkila *et al.*, Nucl. Instrum. Methods A **595**, 637 (2008).

[36] D. Radford (2001), http://radware.phy.ornl.gov/.

[37] P. G. Varmette *et al.*, Phys. Lett. **B410**, 103 (1997).

[38] F. Hannachi, G. Bastin, M. G. Porquet, J. P. Thibaud, C. Bourgeois, L. Hildingsson, N. Perrin, H. Sergolle, F. A. Beck, and J. C. Merdinger, Z. Phys. A **330**, 15 (1988).

[39] M. J. A. de Voigt, R. Kaczarowski, H. J. Riezebos, R. F. Noorman, J. C. Bacelar, M. A. Deleplanque, R. M. Diamond, and F. S. Stephens, Nucl. Phys. **A507**, 447 (1990).

[40] J. Nyberg *et al.*, Nucl. Phys. **A511**, 92 (1990).

[41] G. J. Lane, G. D. Dracoulis, A. P. Byrne, S. S. Anderssen, P. M. Davidson, B. Fabricius, T. Kibedi, A. E. Stuchbery, and A. M. Baxter, Nucl. Phys. **A589**, 129 (1995).

[42] G. D. Dracoulis, A. E. Stuchbery, A. P. Byrne, A. R. Poletti, S. J. Poletti, J. Gerl, and R. A. Bark, J. Phys. G: Nucl. Part. Phys. **12**, L97 (1986).

[43] G. D. Dracoulis, A. P. Byrne, and A. M. Baxter, Phys. Lett. **B432**, 37 (1998).

[44] D. P. McNabb *et al.*, Phys. Rev. C **56**, 2474 (1997).

[45] B. Fant *et al.*, J. Phys. G: Nucl. Part. Phys. **17**, 319 (1991).

[46] G. Baldsiefen, H. Hübel, W. Korten, U. J. van Severen, J. A. Cizewski, N. H. Medina, D. R. Napoli, C. Rossi Alvarez, G. Lo Bianco, and S. Signorelli, Z. Phys. A **355**, 337 (1996).

[47] A. Görgen *et al.*, Nucl. Phys. **A638**, 108 (2001).

[48] X. Sun, U. Rosengård, H. Grawe, H. Haas, H. Kluge, A. Kuhnert, and K. H. Maier, Z. Phys. A **333**, 281 (1989).

[49] J. J. Van Ruyven, J. Penninga, W. H. A. Hesselink, P. Van Nes, K. Allaart, E. J. Hengeveld, H. Verheul, M. J. A. de Voigt, Z. Sujkowski, and J. Blomqvist, Nucl. Phys. **A449**, 579 (1986).

[50] A. N. Andreyev *et al.*, Eur. Phys. J. A **6**, 381 (1999).

[51] K. Van de Vel *et al.*, Eur. Phys. J. A **24**, 57 (2005).

[52] M. Kaci *et al.*, Z. Phys. A **354**, 267 (1996).

[53] B. Cederwall *et al.*, Phys. Lett. **B443**, 69 (1998).

[54] A. N. Andreyev *et al.*, Phys. Rev. C **66**, 014313 (2002).